Available online at www.sciencedirect.com
ScienceDirect
Journal of Solid State Chemistry 180 (2007) 3296–3301
JOURNAL OF SOLID STATE CHEMISTRY
www.elsevier.com/locate/jssc

"Unusual Ln^{3+} substitutional defects": The local chemical environment of Pr^{3+} and Nd^{3+} in nanocrystalline TiO_2 by Ln–K edge EXAFS

Paolo Ghigna[a,*], Adolfo Speghini[b], Marco Bettinelli[b]

[a]Dipartimento di Chimica Fisica "M. Rolla", Università di Pavia, Viale Taramelli 16, I-27100 Pavia, Italy
[b]Dipartimento Scientifico e Tecnologico, Università di Verona and INSTM, UdR Verona, Ca' Vignal, Strada Le Grazie 15, I-37134 Verona, Italy

Received 12 July 2007; received in revised form 3 September 2007; accepted 24 September 2007
Available online 23 October 2007

Abstract

The local chemical environment of the trivalent lanthanide cations in anatase TiO_2 nanopowders doped with 1 mol% of Pr or Nd, prepared via a sol–gel technique, has been studied by means of EXAFS at the Pr and Nd–K edge. Titanium dioxide can be considered an "unusual" host for doping with Ln^{3+} ions due to the large mismatch of both charge and ionic radii between the dopant and the host constituent cations. However, it can be demonstrated that the lanthanide ions enter the anatase structure as substitutional defects with respect to Ti, but that the amount of disorder around the substitutional defects is very large. For both Pr^{3+} and Nd^{3+} ions, the Ln–O and Ln–Ti distances have been found to increase by about 0.45 Å, with respect to what is found for the Ti–O and Ti–Ti distances in pure anatase. Valence-bond calculations have been used to validate the Ln–O distances obtained by the EXAFS fitting. Finally, no evidences for oxygen vacancies clustering around the substitutional defects have been found. Luminescence spectroscopy has shown that the lanthanide ions do not segregate in oxide or pyrochlore impurities phases.

Keywords: TiO_2; Nanocrystalline oxides; Lanthanides; EXAFS; Luminescence

1. Introduction

Crystalline oxide materials doped with trivalent lanthanide ions, which show narrow bandwidth emission spectra in the ultraviolet, visible and infrared ranges, have become very important in the last few years, as they have very useful applications as phosphors for lighting devices and cathode ray tubes, X-ray scintillators and materials which emit light at lower wavelength with respect to that of the exciting radiation (upconversion phenomena). It is worth noting that the local geometry, in particular of the first coordination sphere, has a remarkable importance in determining the spectroscopic properties of the Ln^{3+} ion incorporated in the host matrix. In fact [1–4]:

1. The geometry around the ion determines the splitting of the transitions between multiplets due to the crystal field and therefore the fine structure of the bands depends on the local structure.
2. The intensities of the electric dipole *f–f* transitions (which are usually observed) depend on the degree of distortion of the site accommodating the Ln^{3+} ion, as predicted by the Judd–Ofelt theory [2].
3. The distances between the Ln^{3+} ion and the first neighbours are related to the degree of covalence of the chemical bond, which in turn influences the position of the *f–f* transition (nephelauxetic effect) [3].

In many host matrices, the Ln^{3+} ions occupy well-defined substitutional sites, as can be explained from simple arguments based on the charge and the size of the doping and the substituted ions. Unambiguous examples of this behaviour are the well-known YVO_4, YPO_4 and Y_2SiO_5 luminescent crystals, where the dopant Ln^{3+} ions are accommodated in the Y^{3+} site [5–7]. On the other hand, many cases are reported where the Ln^{3+} impurity has no obvious substitutional site available, namely a site occupied by an ion with similar charge and size. Notable examples of

*Corresponding author. Fax: +39 0382 987575.
E-mail address: paolo.ghigna@unipv.it (P. Ghigna).

0022-4596/$ - see front matter © 2007 Elsevier Inc. All rights reserved.
doi:10.1016/j.jssc.2007.09.025

this behaviour are those involving the nonlinear hosts $LiNbO_3$ [8] and $Sr_xBa_{1-x}Nb_2O_6$ (SBN) [9], which are of great interest for their ability to generate the second harmonic of the light emitted from Ln^{3+} ions. It is worth noting that for these niobate hosts the doping Ln^{3+} ions have a different charge with respect to the host cations (Li^+, Sr^{2+}, Ba^{2+} and formally Nb^{5+}) and also a different ionic radius (the Sr^{2+} and Ba^{2+} cations are larger while the Li^+ and Nb^{5+} are smaller than the Ln^{3+} ions [10]). It is clear that in such cases the local structure around the impurities is not easily predictable from simple arguments and the simultaneous occupation of multiple substitutional sites cannot be a priori ruled out; for instance in SBN, possible occupation of four cationic sites has been proposed [11]. Also simple oxides like TiO_2 or Nb_2O_5, in which a single cationic site is present, are characterised by similar problems due to large mismatch of both charge and ionic radii between the doping Ln^{3+} ions and the host constituent cations. However, recent investigations by our research group have demonstrated the feasibility of the synthesis of both Ln doped TiO_2 [12] and Nb_2O_5 [13] using solution methods. We can refer to Ln doping in host such as $LiNbO_3$, SBN, TiO_2 and Nb_2O_5 as "unusual Ln substitution". Investigating the local structure of the site or sites occupied by the dopant ions is indeed of great relevance for characterising the luminescence properties of these materials. The interest towards nanocrystalline TiO_2 in the anatase form doped with lanthanide ions is also due to the fact that this class of materials finds important applications in the field of photocatalytic degradation of numerous organic molecules [12,14,15]. Moreover, titanium dioxide is considered a non-toxic compound and for this reason it is interesting to investigate the possibility of developing nanocrystalline luminescent TiO_2 activated with lanthanide ions for use in the field of optical imaging for biomedical purposes [16]. Aim of this work is therefore to investigate the local chemical environment of Pr^{3+} and Nd^{3+} substitutional defects in one of such "unusual Ln substituted" oxides, namely TiO_2, by means of a local probe such as EXAFS (extended X-ray absorption fine structure), performed at the Ln–K edges. In addition, the luminescence spectra of Nd^{3+} doped TiO_2 compared with neodymium oxide and neodymium titanate samples allowed to exclude the possibility of phase segregation of the dopant in the anatase sample, thus adding further reliability to the EXAFS data analysis.

2. Experimental details

2.1. Samples preparation

The synthesis of nanocrystalline anatase TiO_2 doped with 1 mol% of trivalent lanthanide ions with respect to Ti has already been described elsewhere [12]. The starting reagents were titanium(IV) butoxide (Aldrich, 97%), $Ln(NO)_3 \cdot 5H_2O$, Ln = Nd, Pr (Aldrich, 99.9%), absolute ethanol and HCl (37%). Briefly, 30.0 ml of ethanol, 0.8 ml of HCl, 6.0 ml of titanium(IV) butoxide and an appropriate amount of the lanthanide nitrate were mixed and stirred for 4 h. The solvent was evaporated at 333 K until the xerogel was formed. The obtained xerogel was heat treated at 773 K for 5 h. The molar ratio between the titanium and the lanthanide ion was 99:1. Moreover, from the broadening of the diffraction peaks and the electron microscopy images, the average size of the nanoparticles is estimated to be about 10–12 nm [12]. An $Nd_2Ti_2O_7$ bulk sample was prepared by solid-state reaction, firing at 1400 °C for 48 h a stoichiometric mixture of TiO_2 (Aldrich 99.9%) and Nd_2O_3 (Aldrich, +99%) previously mixed by stirring overnight an acetone suspension and pressed to pellets. The $Nd_2Ti_2O_7$ sample was checked for phase purity using X-ray powder diffraction (XRPD). The diffraction patterns were collected using a Brucker D8 diffractometer, equipped with a Cu anticathode, an incident slit of 0.5°, an antiscatter slit of 0.5°, a detector slit of 1 mm, and a graphite monochromator in the diffracted beam. Emission spectrum and decay curve for neodymium oxide were performed on a commercial Nd_2O_3 sample (Aldrich, 99.9%).

2.2. EXAFS

The EXAFS spectra were collected at the Nd and Pr–K edges at the BM-29 beamline of ESRF. The data collection was made at room temperature in the transmission mode using a Si(3 1 1) monochromator. The use of the transmission mode has been made possible due to the high energy of the Ln–K edges: measurements at the Ln–L_{III} edges would have implied the use of fluorescence detection, and thus the interference with the Ti$K\alpha$ and Ti$K\beta$ lines. For the measurement, a proper amount of sample (ca. 0.3 g) intended to give the maximum contrast at the Ln–K edge was thoroughly mixed with cellulose in an agate mortar and pressed to pellet. The data analysis was carried out taking advantage of the EXBACK and EXCURV98 programs [17].

2.3. Luminescence

The emission spectra of the Nd^{3+} doped TiO_2 nanocrystalline sample, and Nd_2O_3 powders (Aldrich, 99.9%) were measured upon excitation with the third harmonic (at 355 nm) of the fundamental radiation of a pulsed Nd-YAG laser. The emission radiation was dispersed with a half-meter monochromator equipped with a 150 lines/mm grating. An air-cooled CCD device was employed to measure the emission spectra. The emission decay curves were measured using as the excitation source the third harmonic (at 355 nm) of the fundamental radiation of a pulsed Nd-YAG laser, a GaAs photomultiplier and a digital oscilloscope. All the luminescence measurements were collected at room temperature.

3. Results and discussion

Powder X-ray diffraction shows that the nanocrystalline TiO_2 samples doped with Pr^{3+} and Nd^{3+} are single-phase materials having the anatase structure. The variation of the lattice parameters and volume with respect to undoped TiO_2 anatase has not been investigated in detail for the present samples; however, in the case of nanocrystalline TiO_2:Eu^{3+} (1 mol%), obtained with the same procedure, a Rietveld analysis showed that the unit cell is characterised by a very small increase in volume (of the order of 0.15%) compared to the undoped material. Preliminary measurements of diffuse reflectance absorption spectra measured in the UV–VIS region only evidenced *f–f* transitions attributed to the trivalent dopants. No strong bands indicative of the presence of Ln^{4+} ions were observed.

Figs. 1 and 2 show the Pr–K edge and the Nd–K edge XAFS spectra of the samples investigated in this work. The statistical noise in the $\chi(k)$ was estimated by fitting a straight line on the high energy tail of the absorption spectra, where the EXAFS oscillations are undetectable: for example, for the Pr–K edge spectrum, this has been done at ca. 42,800 eV, which roughly corresponds to $k = 14\,\text{Å}^{-1}$. The noise is, therefore, estimated from the standard deviation of the residual signal which is of the order of 10^{-4} after normalisation for the edge jump.

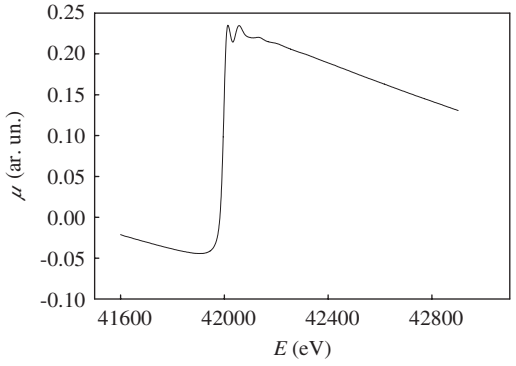

Fig. 1. Pr–K edge XAFS for the Pr^{3+} doped anatase nanocrystalline TiO_2 sample.

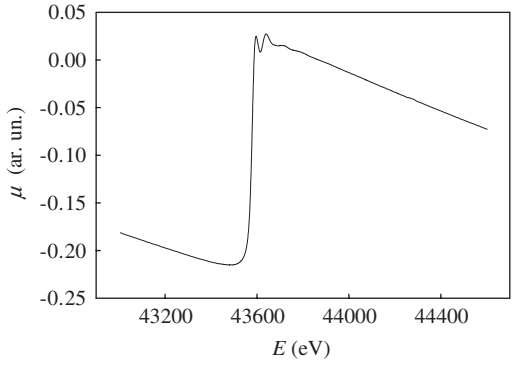

Fig. 2. Nd–K edge XAFS for the Nd^{3+} doped anatase nanocrystalline TiO_2 sample.

Similar results have been obtained for the Nd–K edge spectrum. It is well apparent that the EXAFS oscillations in both spectra are small and rapidly vanishing with increasing energy. This is a clear indication that doping with Ln^{3+} induces a great amount of disorder around the impurity in the anatase structure. Figs. 3 and 4 show the EXAFS signals for the spectra in Figs. 1 and 2, respectively, together with their Fourier transforms (FT). The two spectra look impressively similar, the main difference between the two being the lower resolution in the FT of that at the Nd–K edge (Fig. 4), due to the reduced k range available at this edge. In both spectra, the first peak in the EXAFS FT, i.e. at distances around 2 Å can be attributed to oxygen atoms (nearest neighbours, NN). The weaker peak found close to 3 Å corresponds to the next nearest neighbours (NNN), i.e. to Ti ions. The best fits, according to the structural models reported in Tables 1

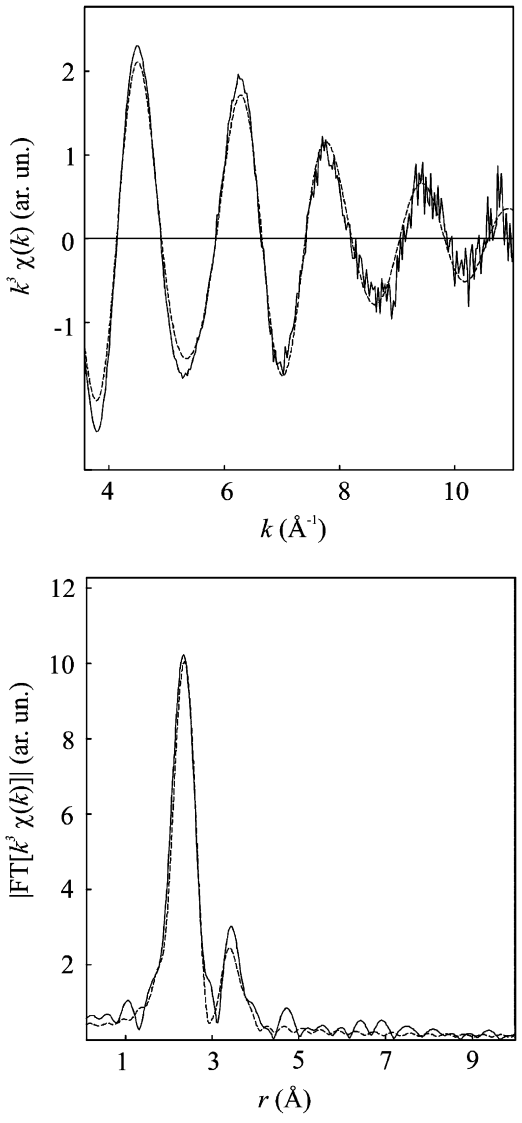

Fig. 3. Upper panel: extracted EXAFS signal from the spectrum of Fig. 1. Lower panel: the corresponding Fourier transform (full lines in both panels). The dashed lines correspond to the fit according to the structural model described in the text.

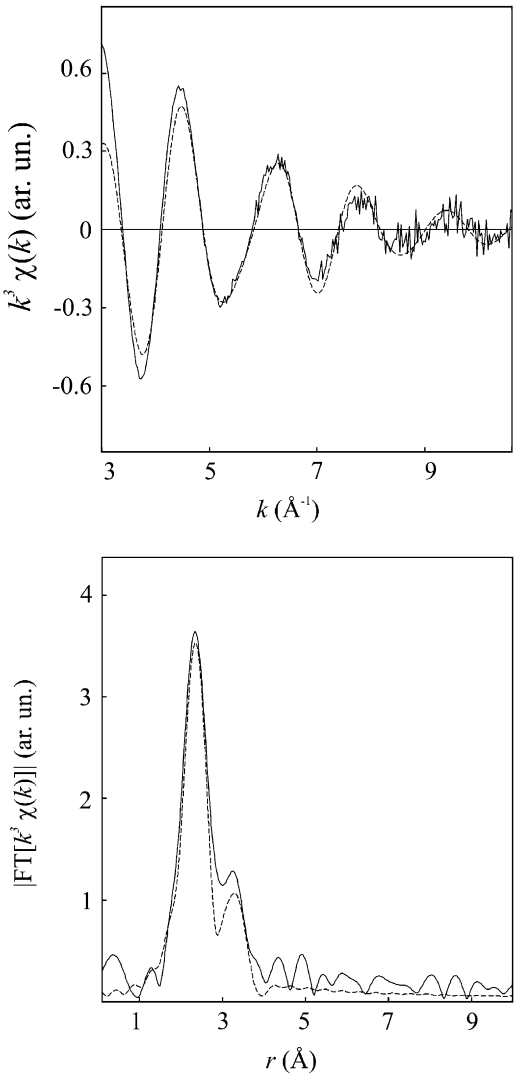

Fig. 4. Upper panel: extracted EXAFS signal from the spectrum of Fig. 2. Lower panel: the corresponding Fourier transform (full lines in both panels). The dashed lines correspond to the fit according to the structural model described in the text.

Table 1
EXAFS fitting parameters for the spectrum of Fig. 3 (Pr^{3+} doped TiO_2)

Shell	Atom	r (Å)	σ^2 (Å^2)	r_0 (Å)
1 (six neighbours)	O	2.400(5)	0.0107(3)	1.947
2 (four neighbours)	Ti	3.38(1)	0.023(2)	3.04

r: Distances; σ^2: distance variances (Debye–Waller factors); for comparison, the distances Ti-neighbours in anatase, calculated from the pertinent lattice constants are reported as r_0; in the case of the Ti–O distance, the reported value is a average of the four "equatorial" distances (1.933 Å) and the two "axial" distances (1.976 Å).

and 2, for the Pr–K edge spectrum and the Nd–K edge spectrum, respectively, are shown in Figs. 3 and 4 as dotted lines. According to the data reported in Tables 1 and 2, the local chemical environments of Pr^{3+} and Nd^{3+} in the anatase host look impressively similar. In addition, it is

Table 2
EXAFS fitting parameters for the spectrum of Fig. 4 (Nd^{3+} doped TiO_2)

Shell	Atom	r (Å)	σ^2 (Å^2)	r_0 (Å)
1 (six neighbours)	O	2.394(9)	0.0113(6)	1.947
2 (four neighbours)	Ti	3.34(2)	0.023(2)	3.04

r: Distances; σ^2: distance variances (Debye–Waller factors); for comparison, the distances Ti-neighbours in anatase, calculated from the pertinent lattice constants are reported as r_0; in the case of the Ti–O distance, the reported value is a average of the four "equatorial" distances (1.933 Å) and the two "axial" distances (1.976 Å).

clear that by comparing the Ln^{3+}-neighbours distances with the crystallographic values for the corresponding Ti-neighbours distances, the Ln^{3+} doping induces a massive local change of the anatase structure: this is in nice agreement with the presence of a great amount of disorder which is at a glance deduced from the spectra (as anticipated above) and confirmed by large values of the σ^2 parameters. It should be noticed that the models used for the EXAFS fitting implicitly assumed that the Ln^{3+} ions enter into the anatase structure as substitutional defects on the Ti position. An independent confirmation of this assumption can be obtained by bond-valence calculations [18]. Using the Ln^{3+}–O distances reported in Tables 1 and 2, and 6 as the coordination number, the calculated charges on Pr and Nd are 2.96 and 2.75, respectively, that are both in good agreement with the formal (III) oxidation state of both cations. Thereof, by the EXAFS analysis, we obtained no evidence of clustering of possible oxygen vacancies that can be formed for charge compensating the Ln_{Ti} defects around them. As a final comment on the fitting procedure reported in this work, we could point out that we used the simplest model that is able to give a reasonable account for all of the spectral features which are found in the EXAFS, without introducing unnecessary correlations between the fitting parameters. We are well aware (for example) of the fact that the implicit assumption of a Gaussian distribution function around the dopants is probably not correct due to the large amount of disorder, but in any case, trying to fit the spectra with other distribution functions introduces heavy correlations between, for example, the skewness and the distance and the kurtosis and σ^2. Therefore, these fits are not trustable: the reason for this is probably that the k range available is quite limited.

It can be interesting to compare the results of the present work with those of recent investigations on lanthanide doped TiO_2 samples [19,20]. A XAS investigation on Er doped TiO_2 films [19] revealed that probably a clustering of Er occurs in these films. However, in our case, trying to replace part or the Ti atoms in the second coordination shell with some Pr or Nd did not improve significantly the quality of the fits, and therefore we are more prone to conclude that no clustering of the substitutional defects occur in our samples. This disagreement could be explained by the much higher (15%, cation ratio) doping levels used

in Ref. [19], if compared to those of the present work (1%, cation ratio). Our results seem to be more directly comparable with those of Ref. [20], in which the local chemical environment of Nd doped TiO_2 nanoparticles synthesised by chemical vapour deposition has been studied by means of Nd–L_3 edge XAFS. In that work it has been found that for doping levels around 1–1.5% (cation ratio) Nd enters the TiO_2 anatase structure, but the local structure around the dopants is more similar to that of rutile than that of anatase [20]. It should be noticed, however, that in Ref. [20], the Nd–O and Nd–Ti distances are found to increase by 0.5–0.8 Å, that is, a much larger value than that observed for the present materials (see Tables 1 and 2). It is therefore possible that different preparation methods are able to stabilise different local structures around the lanthanide ions in Ln doped TiO_2. In order to check the possible presence of segregated lanthanide oxide or lanthanum titanate phases (in particular a pyrochlore $Ln_2Ti_2O_7$ phase), we investigated the luminescence spectroscopy of the Nd^{3+} doped TiO_2 nanocrystalline sample and compared it with the spectroscopy of $Nd_2Ti_2O_7$ (prepared by the solid-state technique, see Section 2) and a commercial Nd_2O_3 samples. The room temperature emission spectra of these three samples, measured upon excitation at 355 nm, are shown in Fig. 5. The emission bands around 900 nm are attributed to transitions between the Stark components of the $^4F_{3/2}$ and $^4I_{15/2}$ levels of the Nd^{3+} ions [21]. From Fig. 5, it can be noted that the emission spectra for the Nd^{3+} doped TiO_2 nanocrystalline sample, the $Nd_2Ti_2O_7$ and Nd_2O_3 samples are very different, both in the peak positions and the relative intensity of the bands. Room temperature emission decay curves of the Nd^{3+} doped TiO_2 nanocrystalline sample, the $Nd_2Ti_2O_7$ and Nd_2O_3 samples obtained upon excitation at 355 nm are shown in Fig. 6. All the emission curves have a clear non-exponential behaviour. This is expected in the case of the $Nd_2Ti_2O_7$ and Nd_2O_3 samples, due to the presence of significant cross-relaxation and energy transfer processes between the Nd^{3+} ions. The non-exponential behaviour for the TiO_2 nanocrystalline sample suggests the presence of a significant disorder of the local environment of the lanthanide ions as found in many cases for Ln^{3+} doped glasses [22]. From the emission decay curves, we calculated the effective emission decay times, τ_{eff} using the equation [23]:

$$\tau_{eff} = \frac{\int tI(t)\,dt}{\int I(t)\,dt},$$

where $I(t)$ represents the luminescence intensity at time t corrected for the background and the integrals are evaluated in a range $0 < t < t_{max}$ where $t_{max} \gg \tau_{eff}$. The τ_{eff} values are 91, 9 and 13 μs for the Nd^{3+} doped TiO_2, the

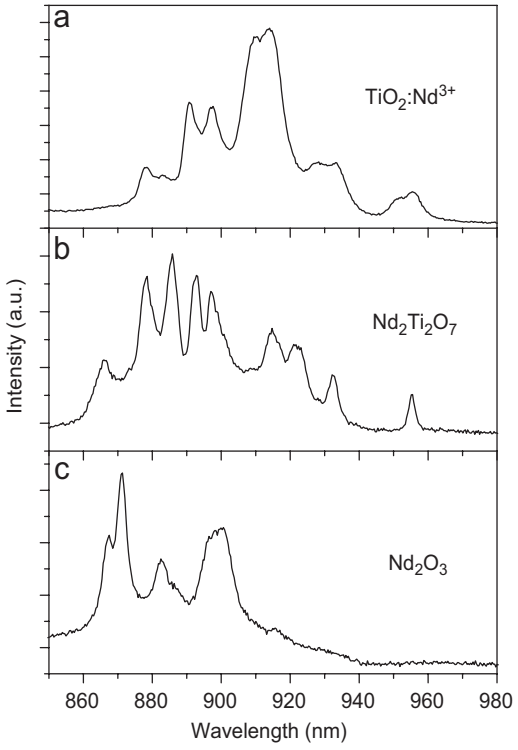

Fig. 5. Room temperature emission spectra of the Nd^{3+} doped TiO_2 nanocrystalline sample (a), the $Nd_2Ti_2O_7$ sample (b) and a commercial Nd_2O_3 sample (c) ($\lambda_{exc} = 355$ nm).

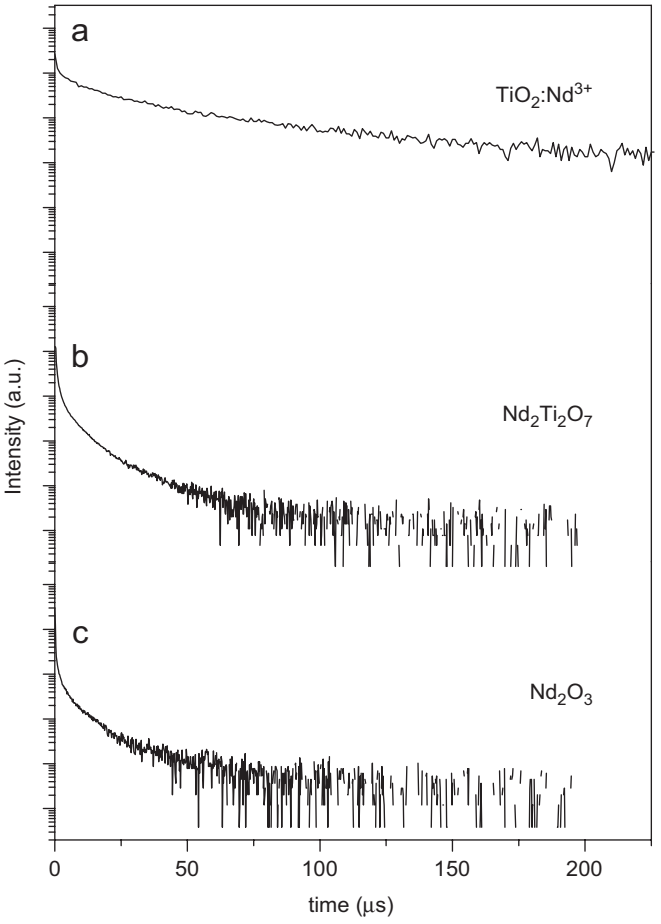

Fig. 6. Room temperature emission decay of a Nd^{3+} doped TiO_2 nanocrystalline sample (a), the $Nd_2Ti_2O_7$ sample (b) and a commercial Nd_2O_3 sample (c) ($\lambda_{exc} = 355$ nm, $\lambda_{em} = 905$ nm).

$Nd_2Ti_2O_7$ and the Nd_2O_3 samples, respectively. We point out that the effective decay time value for the Nd^{3+} doped TiO_2 nanocrystalline sample is about nine times longer than the one for the commercial neodymium oxide. Therefore, these emission results clearly indicate that segregation of the Nd_2O_3 is not present in the Nd^{3+} doped TiO_2 nanocrystalline sample. This is consistent with the EXAFS results, as they clearly show the presence of Ti atoms in the second coordination shell of the Nd^{3+} and Pr^{3+} lanthanide ions (see Figs. 3 and 4). This behaviour is similar to that found for an Er^{3+} doped anatase TiO_2 nanocrystalline sample prepared by a hydrothermal synthesis, reported by Jeon and Braun [24]. In fact, for this latter case, the authors evidenced that the Er^{3+} ions were not present as segregated erbium oxide Er_2O_3. Since the Pr^{3+} and Nd^{3+} ions have a very similar ionic radius and chemistry behaviour, and they show similar EXAFS results (see Tables 1 and 2), it is plausible that also the Pr^{3+} ions are not present as segregated praseodymium oxide. Moreover, a comparison between the emission spectra, emission decay curves and effective lifetimes of the Nd^{3+} doped TiO_2 and the $Nd_2Ti_2O_7$ samples clearly indicate that the pyrochlore phase is not present in the nanocrystalline sample.

4. Conclusions

The local chemical environment of the trivalent lanthanide cations in anatase TiO_2 nanopowders doped with 1 mol% of Pr or Nd with respect to Ti, prepared via the sol–gel technique, has been studied by means of EXAFS at the Pr and Nd–K edge. It can be demonstrated that the Ln^{3+} cations enter the anatase structure as substitutional defects with respect to Ti. However, due to the large difference in ionic radii between Ti^{4+} (0.605 Å, in six-fold coordination [10]) and the Ln^{3+} cations (0.99 and 0.983 Å, for Pr and Nd, respectively, in six-fold coordination [10]), the amount of disorder around the substitutional defects is very large. The EXAFS spectra could be fitted by a two-shell model made up by six oxygens (NN) and four Ti (NNN). For both the dopants, the Ln–NN and Ln–NNN distances have been found to increase of ca. 0.45 Å, if compared to their counterparts in the pure TiO_2 anatase structure. No evidences for oxygen vacancies clustering around the substitutional defects have been found. The values obtained for the Ln–NN distances have been validated by means of bond-valence calculations. We point out that the present results are in good agreement with the luminescence data [12], which show that in the sol–gel prepared nanocrystalline TiO_2 the local structure at the Ln^{3+} cations is affected by strong disorder that broadens the emission features. The comparison of the luminescence spectra and decay curves of the Nd^{3+} doped TiO_2 nanocrystalline sample, of neodymium oxide and neodymium titanate samples indicates that segregation of $Nd_2Ti_2O_7$ or Nd_2O_3 phases in the anatase TiO_2 sample is not present, confirming the EXAFS data analysis.

Acknowledgments

This work has been supported by the European Synchrotron Radiation Facility (ESRF, experiment CH 1965 at the BM29 beamline). The BM29 staff, and in particular Simone de Panfilis, is gratefully acknowledged for help during the XAS data collection. Daniele Falcomer (University of Verona) is gratefully acknowledged for the preparation of the TiO_2 samples.

References

[1] S. Hufner, Optical Spectra of Transparent Rare Earth Compounds, Academic Press, New York, 1978.
[2] R.D. Peacock, The intensities of lanthanide f–f transitions, in: Structure and Bonding, Berlin, vol. 22, 1975, p. 83.
[3] R. Reisfeld, Spectra and energy transfer of rare earths in inorganic glasses, in: Structure and Bonding, Berlin, vol. 13, 1973, p. 53.
[4] J. Holsa, E. Antic-Fidancev, M. Lastusaari, A. Lupei, J. Solid State Chem. 171 (2003) 282.
[5] J.A. Capobianco, P. Kabro, F.S. Ermeneux, R. Moncorge, M. Bettinelli, E. Cavalli, Chem. Phys. 214 (1997) 329.
[6] P.C. Becker, T. Hayhurst, G. Shalimoff, J.G. Conway, N. Edelstein, L.A. Boatner, M.M. Abraham, J. Chem. Phys. 81 (1984) 2872.
[7] J. Shmulovich, G.W. Berkstresser, C.D. Brandle, A. Valentino, J. Electrochem. Soc. 135 (1988) 3141.
[8] A. Lorenzo, H. Jaffrezic, B. Roux, G. Boulon, J. Garcia-Sole, Appl. Phys. Lett. 67 (1995) 3735.
[9] M.O. Ramirez, D. Jaque, L. Ivleva, L.E. Bausa, J. Appl. Phys. 95 (2004) 6185.
[10] R.D. Shannon, C.T. Prewitt, Acta Crystallogr. B 25 (1969) 925.
[11] M.O. Ramirez, L.E. Bausa, A. Speghini, M. Bettinelli, L. Ivleva, J. Garcia Sole, Phys. Rev. B 73 (2006) 035119.
[12] M. Bettinelli, A. Speghini, D. Falcomer, M. Daldosso, V. Dallacasa, L. Romano, J. Phys. Condens. Matter 18 (2006) S2149–S2160.
[13] D. Falcomer, A. Speghini, G. Ibba, S. Enzo, C. Cannas, A. Musinu, M. Bettinelli, J. Nanomater., in press.
[14] U. Diebold, Surf. Sci. Rep. 48 (2003) 53.
[15] D. Falcomer, M. Daldosso, C. Cannas, A. Musinu, B. Lasio, S. Enzo, A. Speghini, M. Bettinelli, J. Solid State Chem. 179 (2006) 2452.
[16] A. Sbarbati, et al., in preparation.
[17] N. Binsted, S.J. Gurman, T.C. Campbell, P.C. Stephenson, EXCURV98 Program, SERC Daresbury Laboratory, Daresbury, 1998.
[18] I.D. Brown, D. Altermatt, Acta Crystallogr. B 41 (1985) 244.
[19] C. Mignotte, J. Non-Cryst. Solids 291 (2001) 56.
[20] W. Li, A.I. Frenkel, J.C. Woicik, C. Ni, S. Ismat Shah, Phys. Rev. B 72 (2005) 155315.
[21] A.A. Kaminskii, Laser Crystals, Springer, Berlin, 1990.
[22] C. Brecher, R.A. Riseberg, Phys. Rev. B 13 (1976) 81.
[23] E. Nakazawa, in: S. Shionoya, W.M. Yen (Eds.), Phosphor Handbook, CRC Press, Boca Raton, FL, 1999, p. 104.
[24] S. Jeon, P.V. Braun, Chem. Mater. 15 (2003) 1256.